JOURNAL OF SOLID STATE CHEMISTRY **139,** 135–143 (1998)
ARTICLE NO. SC987821

High-Temperature Powder Neutron Diffraction Study of the Oxide Ion Conductor $La_{0.9}Sr_{0.1}Ga_{0.8}Mg_{0.2}O_{2.85}$

P. R. Slater,* J. T. S. Irvine,*,[1] T. Ishihara,† and Y. Takita†

*School of Chemistry, University of St. Andrews, St. Andrews, Fife KY16 9ST, United Kingdom; and †Department of Applied Chemistry, Oita University, Dannoharu 700, Oita 870-11, Japan

Received November 13, 1997; in revised form March 5, 1998; accepted March 17, 1998

Powder neutron diffraction data have been collected between room temperature and 1000°C for the oxide ion conductor $La_{0.9}Sr_{0.1}Ga_{0.8}Mg_{0.2}O_{2.85}$ and the undoped parent phase $LaGaO_3$. In agreement with previous studies, refinement of the data for the undoped phase showed that the cell is orthorhombic (*Pbnm*) at room temperature and rhombohedral (*R*3*c*) between 250 and 1000°C. The structure of the doped system $La_{0.9}Sr_{0.1}Ga_{0.8}Mg_{0.2}O_{2.85}$ is, however, significantly different from that of pure $LaGaO_3$. The room temperature structure is monoclinic (*I*2/*a*), and there appear to be two phase transitions between 250 and 1000°C: monoclinic (pseudo-orthorhombic) → monoclinic (pseudo-rhombohedral) → rhombohedral. Significant changes are also seen in the GaO_6 octahedra on doping $LaGaO_3$. In particular, the octahedra are substantially more distorted in the doped phase. The tilting of the octahedra is smaller for the doped phase and the degree of tilting is reduced as the temperature is raised. Possible correlation between the tilting of the octahedra and the activation energy for oxide ion conduction is presented.

INTRODUCTION

There is a growing need for more environmentally friendly and efficient means of energy conversion. At the forefront of this is the solid oxide fuel cell (SOFC), which it is hoped will find widespread application in the conversion of chemical to electrical energy. One of the problems of this cell is the high temperature (1000°C) required to obtain reasonable oxide ion conduction for the electrolyte, currently yttria-stabilized zirconia (YSZ). Although there are technological advantages to high-temperature operation, it does place constraints on materials selection and on the lifetime of the fuel cell. Recently, Ishihara *et al.* have reported high oxide ion conductivity in the perovskite system $LaGaO_3$ doped with Sr on the La site and Mg on the Ga site (1, 2). The oxide ion conductivity at 850°C for the composition $La_{0.9}Sr_{0.1}Ga_{0.8}Mg_{0.2}O_{2.85}$ is similar to that of YSZ at 1000°C. Use of this electrolyte would therefore allow a lower fuel cell operation temperature. Fuel cell operation has indeed been demonstrated at lower temperatures using this material as the electrolyte (3, 4)

A significant amount of further work is, however, needed to fully characterize this material, particularly since the origin of the very high oxide ion conductivity in this system is still subject to speculation. To this end, structural data are vital in distinguishing the crucial features of this system. So far structural data on the doped system have been very limited. There have been a number of studies of $LaGaO_3$ (5–7), but the only structural data on the doped phase have been room temperature data by X-ray diffraction (8). $LaGaO_3$ has a distorted perovskite structure with tilting of the GaO_6 octahedra (Fig. 1), resulting in an orthorhombic cell at room temperature. At a temperature around 150°C the cell transforms to rhombohedral symmetry (7).

Since there have been no systematic studies of the changes in the structure of this high oxide ion conductor as the temperature is raised, we have performed a comprehensive structural study by powder neutron diffraction of both the doped and undoped phases, in an attempt to find a correlation between the structural features and the high ionic conductivity. Powder neutron diffraction data were collected between 25 and 1000°C for both $LaGaO_3$ and $La_{0.9}Sr_{0.1}Ga_{0.8}Mg_{0.2}O_{2.85}$, and the results, showing significant differences between the two systems, are reported here.

EXPERIMENTAL

$LaGaO_3$ and $La_{0.9}Sr_{0.1}Ga_{0.8}Mg_{0.2}O_{2.85}$ were prepared from high-purity La_2O_3, $SrCO_3$, Ga_2O_3, and MgO. Stoichiometric amounts were ball-milled and then precalcined at 1000°C for 6 hr. The resulting powder was reground and then heated to 1500°C for 6 hr. Time-of-flight powder neutron diffraction data were collected on diffractometer

[1] To whom correspondence should be addressed. Fax: (01334) 463808. E-mail: jtsi@st-and.ac.uk.

0022-4596/98 $25.00

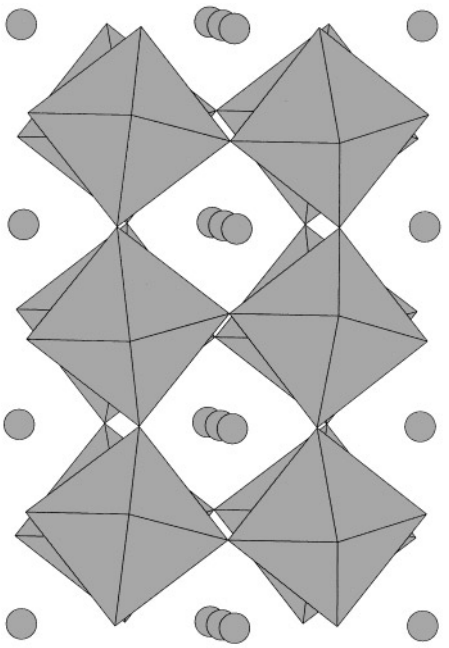

FIG 1. Structure of $LaGaO_3$ showing tilting of GaO_6 octahedra.

HRPD, ISIS, Rutherford Appleton Laboratory. Data were collected at temperatures of 25, 250, 500, 750, and 1000°C for both samples. Structural refinement was performed by the Rietveld method using the program TF12LS, which is based on the Cambridge Crystallographic Subroutine Library (CCSL) (9, 10). Scattering lengths of 0.827, 0.702, 0.729, 0.5375, and 0.5805 (all $\times 10^{-12}$ cm) were assigned to La, Sr, Ga, Mg, and O, respectively.

STRUCTURE REFINEMENT

The structural data from Marti *et al.* for undoped $LaGaO_3$ (7) were used as initial starting parameters, with the space group *Pbnm* for the orthorhombic symmetry and *R*3*c* for the rhombohedral symmetry (hexagonal setting employed).

Initial refinement of the data indicated that for the undoped $LaGaO_3$ phase the sample was orthorhombic at 25°C and rhombohedral for the other temperature sets. This is in agreement with previous reports (5–7). Structural parameters are presented in Table 1, with the neutron profiles for the 25°C data set shown in Fig. 2. The Ga–O bond distances are given in Table 2.

For the $La_{0.9}Sr_{0.1}Ga_{0.8}Mg_{0.2}O_{2.85}$ sample, there were small amounts of impurities, such as La_4SrO_7, present, since it is very difficult to prepare completely single-phase samples of the doped material. The regions displaying these impurities were therefore excluded in the refinement. Preliminary refinement of the data for $La_{0.9}Sr_{0.1}Ga_{0.8}Mg_{0.2}O_{2.85}$ suggested that in this case the cell was orthorhombic for the temperatures 25 and 250°C and rhombohedral for 500–1000°C inclusive. It was, however, clear from the results that there were some problems associated with these refinements. In particular, the fits of the data were significantly better for the 750 and 1000°C data sets than for the other temperatures, with the 250°C data set showing the worst fit. In addition, the standard deviations of the cell parameters *a* and *b* for the 500°C data set were very high ($\approx$0.2%) and much higher than for the *c* parameter, despite the fact that $c > a,b$ ($a = b = 5.56(1)$, $c = 13.5738(1)$ A). This suggested that there may be some monoclinic distortion of the cell. Therefore a monoclinic cell, *I*2/*a*, was examined for all the data sets. The cell employed was that proposed by Ritter *et al.* for $Pr_{0.6}Sr_{0.4}MnO_3$, which has the space group *Pbnm* at room temperature, changing to monoclinic *I*2/*a* at lower temperature (11). The body-centered cell was in agreement with the systematic absences observed for $La_{0.9}Sr_{0.1}Ga_{0.8}Mg_{0.2}O_{2.85}$. Refinement using the monoclinic cell resulted in improved *R* factors for the 25, 250, and 500°C data sets (R_{wp}/R_e reducing from 3.35 to 2.93 for the 25°C data set, from 3.80 to 2.73 at 250°C, and from

TABLE 1
Refined Structural Parameters for $LaGaO_3$ between 25 and 1000°C

Atom	Parameter	25°C	250°C	500°C	750°C	1000°C
La	*x*	−0.0047(2)	0	0	0	0
	y	−0.0168(2)	0	0	0	0
	z	0.25	0.2508(3)	0.2512(3)	0.2513(3)	0.2517(2)
	ITF	0.39(2)	0.66(2)	0.97(2)	1.30(2)	1.63(3)
	Site	1.0	1.0	1.0	1.0	1.0
Ga	*x*	0.5	0	0	0	0
	y	0	0	0	0	0
	z	0	0	0	0	0
	ITF	0.29(2)	0.46(2)	0.68(2)	0.91(2)	1.10(2)
	Site	1.0	1.0	1.0	1.0	1.0
O1	*x*	0.2705(2)	0.1137(2)	0.1163(3)	0.1192(3)	0.1224(3)
	y	0.2714(2)	0.3420(4)	0.3439(4)	0.3457(4)	0.3473(4)
	z	0.5365(1)	0.0772(2)	0.0768(3)	0.0756(3)	0.0747(2)
	ITF	0.53(2)	0.80(1)	1.19(2)	1.61(2)	2.05(2)
	Site	1.0	1.0	1.0	1.0	1.0
O2	*x*	0.0681(2)				
	y	0.5078(3)				
	z	0.25				
	ITF	0.41(2)				
	Site	1.0				
	a (Å)	5.52432(2)	5.5358(7)	5.5472(8)	5.560(1)	5.5745(8)
	b (Å)	5.49246(2)	5.5358(7)	5.5472(8)	5.560(1)	5.5745(8)
	c (Å)	7.77448(4)	13.39797(6)	13.45131(6)	13.50672(6)	13.56587(7)
	Space group	*Pbnm*	*R*3*c*	*R*3*c*	*R*3*c*	*R*3*c*
	R_I	6.26	5.77	5.93	6.56	6.94
	R_p	5.04	5.12	4.89	4.79	4.55
	R_{wp}	5.89	6.01	5.78	5.70	5.44
	R_e	2.41	2.54	2.52	2.54	2.56

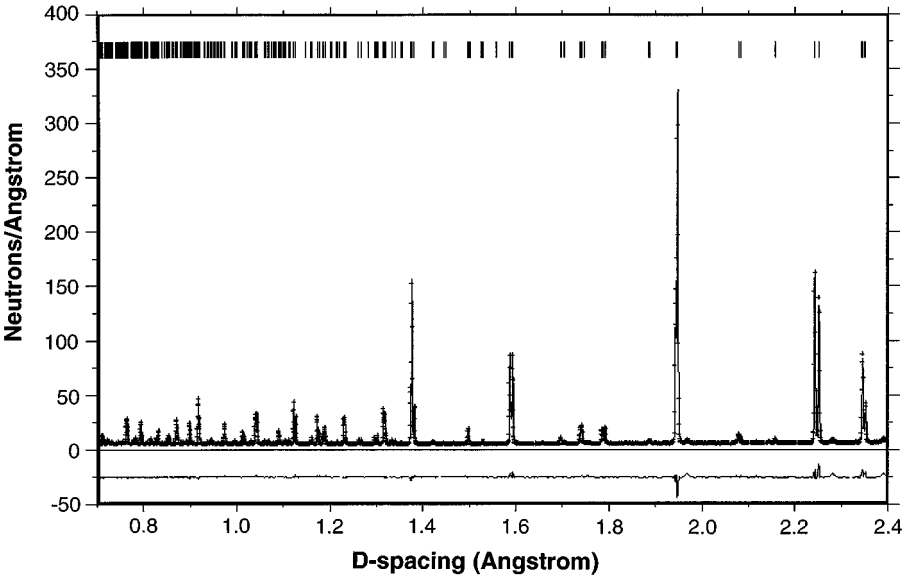

FIG. 2. Observed, calculated, and difference profiles for $LaGaO_3$ at 25°C.

3.17 to 3.02 at 500°C), with the refinements for the 750 and 1000°C data sets being unstable with the monoclinic cell. In Fig. 3 we show the data fits in the region of *d*-spacing 2.24–2.28 for both orthorhombic and monoclinic cell refinements for the 250°C data set. This clearly shows the improved fit associated with the monoclinic cell at this temperature. The reduced *R* factors and the fact that the angle β refined to 90.06–90.07° for the "orthorhombic" samples (25 and 250°C), whereas β refined to 90.15° for the "rhombohedral" sample (500°C) and the standard deviations for the cell parameters of this data set were now reasonable, supported the conclusion that these samples were monoclinic.

In all the $La_{0.9}Sr_{0.1}Ga_{0.8}Mg_{0.2}O_{2.85}$ refinements, the La/Sr site occupancies were fixed at the weighed-out composition (0.9/0.1), while the Ga/Mg and oxygen site occupancies were refined. Fixing the Ga/Mg site occupancy at that weighed out and refining the La/Sr site occupancy gave a similar fit with a La/Sr composition of 0.93(5)/0.07(5) for the 25°C data set. The oxygen site occupancies were also refined. For the monoclinic cells there are two oxygen sites, and for the 25 and 250°C data sets the refinement of the site occupancies indicated oxygen vacancies located only on the O2 (apical) sites. For the 500°C data set, the refinement was stable with the vacancies in either the O1 or O2 sites, and both refinements gave identical fits. Therefore for the final refinement of this temperature set the oxygen sites were fixed at randomly distributed over the two sites. This gave the same fit as the free refinements detailed earlier. The final refined structural data are given in Table 3, with the neutron profiles for the 25°C data set shown in Fig. 4. The Ga–O bond distances are given in Table 4.

Refinement of the $LaGaO_3$ data using a monoclinic cell was also attempted, since for all the samples except the 25°C data set, the standard deviation of the cell parameters was high (Table 1), although substantially lower than observed in the rhombohedral refinement of $La_{0.9}Sr_{0.1}Ga_{0.8}Mg_{0.2}O_{2.85}$ at 500°C. These refinements, however, resulted in no improvement in the fit for any of the data sets, and the angle β refined to 90.0° for the orthorhombic (25°C) sample. Therefore the higher symmetry initial refinements were preferred.

TABLE 2
Variation of Ga–O Bond Distances with Temperature for $LaGaO_3$ (LG)

Bond	25°C	250°C	500°C	750°C	1000°C
Ga–O1 (Å)	1.972(2) [×2]	1.962(2) [×3]	1.972(3) [×3]	1.976(3) [×3]	1.980(3) [×3]
Ga–O1 (Å)	1.978(2) [×2]	1.992(2) [×3]	1.991(3) [×3]	1.997(3) [×3]	2.004(3) [×3]
Ga–O2 (Å)	1.980(1) [×2]				

RESULTS AND DISCUSSION

The structural data show significant differences between $LaGaO_3$ and $La_{0.9}Sr_{0.1}Ga_{0.8}Mg_{0.2}O_{2.85}$, both in their structures at room temperature and in their high-temperature structures. These changes are of fundamental importance in trying to account for the high oxide ion conductivity of the latter, and they will now be discussed in detail.

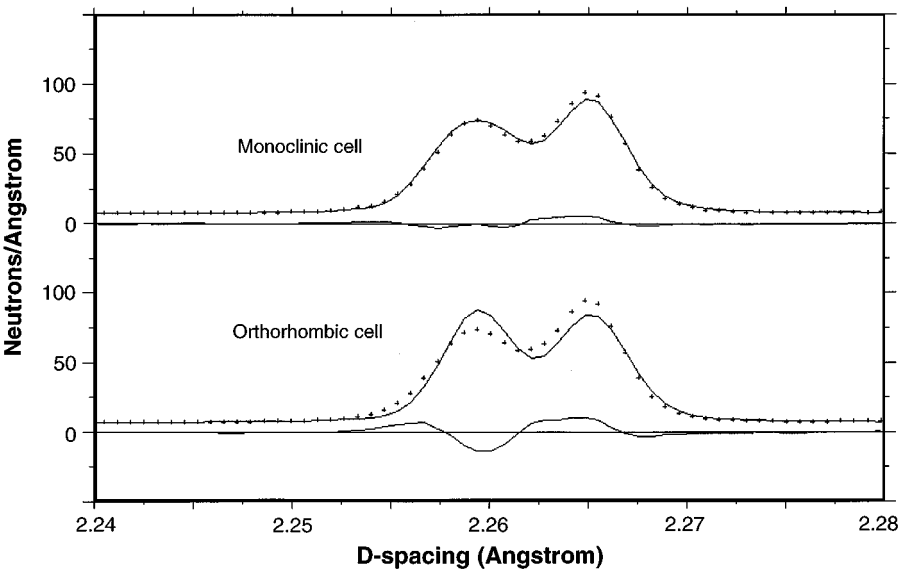

FIG. 3. Observed, calculated, and difference profiles in the *d*-spacing region 2.24–2.28 Å for $La_{0.9}Sr_{0.1}Ga_{0.8}Mg_{0.2}O_{2.85}$ at 250°C showing the fits for the monoclinic and orthorhombic cells.

The refinements of the $LaGaO_3$ data produced results similar to those of previous studies (4–7), with the structure being orthorhombic at room temperature and rhombohedral for the temperature range 250–1000°C. One problem with the refinements for the rhombohedral data sets was the fact that the standard deviations for the cell edges *a* and *b* were high (Table 1). Attempts to refine the data on monoclinic cells produced, however, no improvement in the fit. With respect to this, Kobayashi *et al.* have claimed from high-temperature X-ray diffraction and differential scanning calorimetry studies that the structure between 150 and 1000°C is in fact monoclinic (12). However, between 150 and 750°C the monoclinic distortion is negligible, and so the structure can be viewed as rhombohedral, whereas between 750 and 1000°C the distortion becomes significant. For our data the only evidence for a possible distortion from rhombohedral was the high standard deviations for the *a* and *b* cell edges, and these were high for the whole rhombohedral temperature range 250–1000°C, not just for the temperature range 750–1000°C.

The results for the doped sample, $La_{0.9}Sr_{0.1}Ga_{0.8}Mg_{0.2}O_{2.85}$, proved more complicated than for $LaGaO_3$, fully justifying the study. Initial refinement of the data suggested orthorhombic symmetry for 25–250°C and rhombohedral for 500–1000°C, similar to the results for $LaGaO_3$. However, further refinement of the 25–500°C data sets on monoclinic cells produced improved fits. Therefore, contrary to previous claims (8), the room temperature structure is monoclinic, not orthorhombic. It is not surprising that this monoclinic distortion has been missed previously, as the deviation from orthorhombic symmetry is relatively small, requiring the high resolution of the diffractometer HRPD to resolve. As for the room temperature data, the structure at 250°C is also monoclinic. For both these temperatures the distortion from orthorhombic symmetry is relatively small, $\beta = 90.06$–$90.07°$, and so these structures may be classed as monoclinic (pseudo-orthorhombic). For the 500°C data set the structure involves a small monoclinic distortion from rhombohedral symmetry, and so this may be classed as monoclinic (pseudo-rhombohedral). There thus appear to be two phase transitions for this sample between 25 and 1000°C, namely a monoclinic (pseudo-orthorhombic) → monoclinic (pseudo-rhombohedral), which occurs between 250 and 500°C, and a monoclinic (pseudo-rhombohedral) → rhombohedral transition, which occurs between 500 and 750°C.

Figure 5 shows the changes in unit cell volume per formula unit with temperature. For $LaGaO_3$ there appears to be a clear change in slope of the graph of cell volume per formula unit versus temperature between room temperature and 250°C, in agreement with the structure refinements. For $La_{0.9}Sr_{0.1}Ga_{0.8}Mg_{0.2}O_{2.85}$ it is impossible to distinguish both phase transitions from this plot as we have only five points, but it is clear that significant structural changes are occurring in the region of 500°C. The doped sample shows a volume expansion of 1% over the undoped, which can be partly attributed to the slightly larger ionic radii of Mg^{2+} and Sr^{2+} (13) and, perhaps more importantly, the decreased electrostatic forces due to the high concentration of oxygen vacancies.

TABLE 3
Refined Structural Parameters for $La_{0.9}Sr_{0.1}Ga_{0.8}Mg_{0.2}O_{2.85}$ between 25°C and 1000°C

Atom	Parameter	25°C	250°C	500°C	750°C	1000°C
La/Sr	x	0.25	0.25	0.25	0	0
	y	− 0.0003(6)	0.0028(4)	0.000(1)	0	0
	z	0	0	0	0.2544(6)	0.248(2)
	ITF	1.37(4)	1.74(3)	1.99(5)	2.39(6)	2.8(1)
	Site	0.9/0.1	0.9/0.1	0.9/0.1	0.9/0.1	0.9/0.1
Ga/Mg	x	0	0	0	0	0
	y	0.5	0.5	0.5	0	0
	z	0	0	0	0	0
	ITF	0.72(4)	0.89(4)	1.20(5)	1.47(6)	1.86(8)
	Site	0.80(1)/0.20(1)	0.78(1)/0.22(1)	0.79(1)/0.21(1)	0.79(1)/0.21(1)	0.77(1)/0.23(1)
O1	x	0.4713(3)	0.4736(3)	0.4780(8)	0.1354(9)	0.147(1)
	y	0.7605(5)	0.7619(5)	0.7318(8)	0.346(1)	0.347(2)
	z	0.2465(9)	0.246(1)	0.256(1)	0.084(1)	0.080(2)
	B_{11}	2.2(1)	2.6(1)	6.2(3)	4.7(3)	6.7(4)
	B_{22}	2.9(1)	3.2(1)	2.7(2)	2.0(1)	2.4(3)
	B_{33}	5.2(2)	5.7(2)	3.8(2)	5.7(1)	6.6(3)
	B_{12}	− 2.8(1)	− 2.8(1)	− 2.2(2)	− 1.5(1)	− 1.6(3)
	B_{13}	− 2.4(1)	− 2.2(1)	1.0(2)	0.9(2)	1.4(4)
	B_{23}	0.9(1)	1.3(1)	− 0.4(2)	1.5(2)	1.7(4)
	Site	1.02(2)	1.00(2)	0.95	0.94(2)	0.96(2)
O2	x	0.25	0.25	0.25		
	y	0.4378(5)	0.440(1)	0.443(1)		
	z	0	0	0		
	B_{11}	0.8(2)	0.3(2)	1.8(2)		
	B_{22}	1.1(2)	2.2(2)	2.9(2)		
	B_{33}	2.4(2)	2.6(2)	2.5(2)		
	B_{12}	0.0	0.0	0.0		
	B_{13}	− 1.2(2)	− 1.3(2)	1.1(2)		
	B_{23}	0.0	0.0	0.0		
	Site	0.87(2)	0.84(2)	0.95		
	a (Å)	7.81603(4)	7.83332(5)	7.85603(5)	5.57402(3)	5.59033(3)
	b (Å)	5.53930(2)	5.54993(3)	5.55965(3)	5.57402(3)	5.59033(3)
	c (Å)	5.51467(2)	5.52917(3)	5.54542(3)	13.61871(7)	13.67757(8)
	β (deg)	90.0600(4)	90.0663(5)	90.1542(6)		
	Space group	$I2/a$	$I2/a$	$I2/a$	$R3c$	$R3c$
	R_I	3.09	3.12	3.39	4.22	3.89
	R_p	3.88	3.53	4.05	4.15	4.03
	R_{wp}	4.92	4.53	5.05	5.14	4.34
	R_e	1.68	1.66	1.67	1.73	1.76

In both systems the main distortion of the structure from the ideal perovskite is the tilting of the GaO_6 octahedra, and the symmetry changes observed have a direct effect on this tilting. There are two tilt directions, representing tilting about the $[001]_p$ and $[110]_p$ primitive perovskite directions. For the orthorhombic space group, the tilts occur about the b ($[110]_p$) and c ($[001]_p$) axes and may be represented as $a^0b^+c^+$ (or $a^-a^-c^+$ in terms of the notation of Glazer (14)), which means that the tilts are in phase when successive octahedra along the same axis are considered. For the chosen cell choice in the monoclinic space group, the tilts occur about the c ($[110]_p$) and a ($[001]_p$) axes and may be represented as $a^-b^0c^+$ (or $a^-a^-c^-$ in terms of the notation of Glazer (14) with the axes changed to allow direct comparison with the orthorhombic cell). In this case the $[001]_p$ tilt is now antiphase for successive octahedra. This difference can be seen by close inspection of the two structures looking down the $[001]_p$ axis (Fig. 6). The rhombohedral cell is similar to the monoclinic cell, except that in this case the degrees of tilt about the two axes are equal (in terms of the notation of Glazer, the system is $a^-a^-a^-$ [14]).

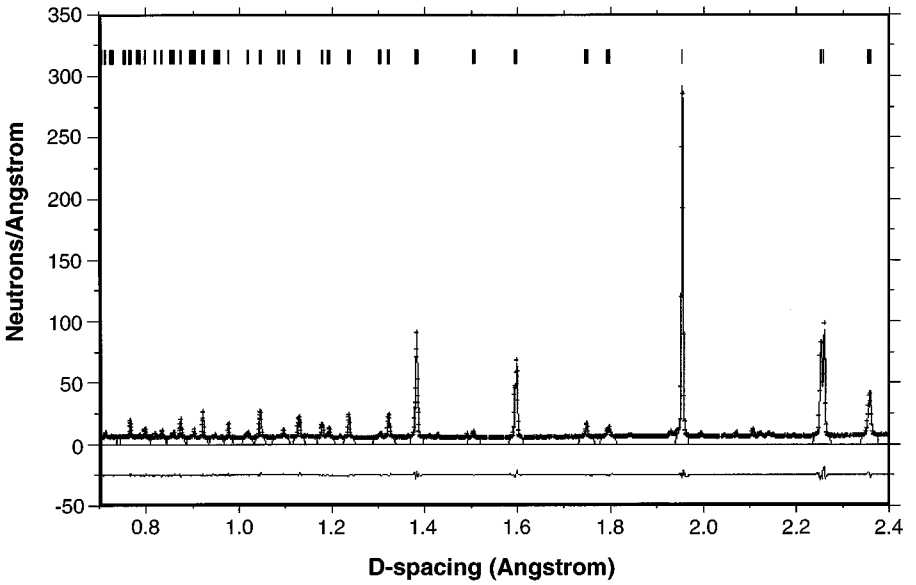

FIG. 4. Observed, calculated, and difference profiles for $La_{0.9}Sr_{0.1}Ga_{0.8}Mg_{0.2}O_{2.85}$ at 25°C.

The degree of tilting of the octahedra is strongly affected by the doping. A significant reduction in the tilting of the octahedra is observed after doping (e.g., at room temperature the $[001]_p$ tilt reduces from 9.6° ($LaGaO_3$) to 6.8° ($La_{0.9}Sr_{0.1}Ga_{0.8}Mg_{0.2}O_{2.85}$), whereas there is a smaller reduction in the $[110]_p$ tilt, from 11° ($LaGaO_3$) to 10° ($La_{0.9}Sr_{0.1}Ga_{0.8}Mg_{0.2}O_{2.85}$). In both systems the tilt angles are reduced as the temperature is raised, although for the doped systems, the change is more significant (Fig. 7). As stated earlier, the two tilt angles become equal when the samples become rhombohedral.

The doping also has a direct effect on the GaO_6 octahedra themselves. In $LaGaO_3$ all the Ga–O bond distances are similar, whereas for $La_{0.9}Sr_{0.1}Ga_{0.8}Mg_{0.2}O_{2.85}$ there is significantly more distortion in the octahedra (Tables 2 and 4). This progresses over the entire temperature range (Fig. 8), although there is evidence for a reduction in the distortion for the 1000°C $La_{0.9}Sr_{0.1}Ga_{0.8}$ $Mg_{0.2}O_{2.85}$ data set, which is almost certainly related to the approach toward cubic symmetry.

TABLE 4
Variation of Ga–O Bond Distances with Temperature for $La_{0.9}Sr_{0.1}Ga_{0.8}Mg_{0.2}O_{2.85}$ (LSGM)

Bond	25°C	250°C	500°C	750°C	1000°C
Ga–O1 (Å)	1.996(4) [×2]	2.002(4) [×2]	2.022(7) [×2]	2.04(1) [×3]	2.02(1) [×3]
Ga–O1 (Å)	1.940(4) [×2]	1.939(4) [×2]	1.924(7) [×2]	1.92(1) [×3]	1.95(1) [×3]
Ga–O2 (Å)	1.984(1) [×2]	1.986(2) [×2]	1.989(2) [×2]		

The oxygen site occupancies for $La_{0.9}Sr_{0.1}Ga_{0.8}Mg_{0.2}$ $O_{2.85}$ (Table 3) show that there is a degree of ordering of the oxygen vacancies at low temperatures, with preferential location of these vacancies on the apical O2 sites of the octahedra at both 25 and 250°C. To achieve high oxide ion conductivity, we require the vacancies to be disordered, and

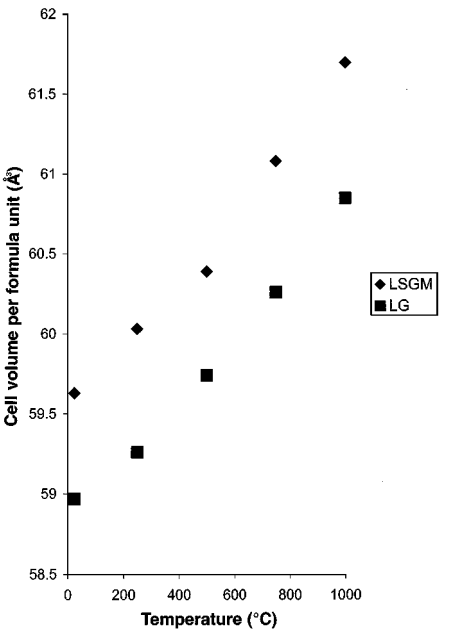

FIG. 5. Plot of cell volume per formula unit versus temperature for $LaGaO_3$ (LG) and $La_{0.9}Sr_{0.1}Ga_{0.8}Mg_{0.2}O_{2.85}$ (LSGM).

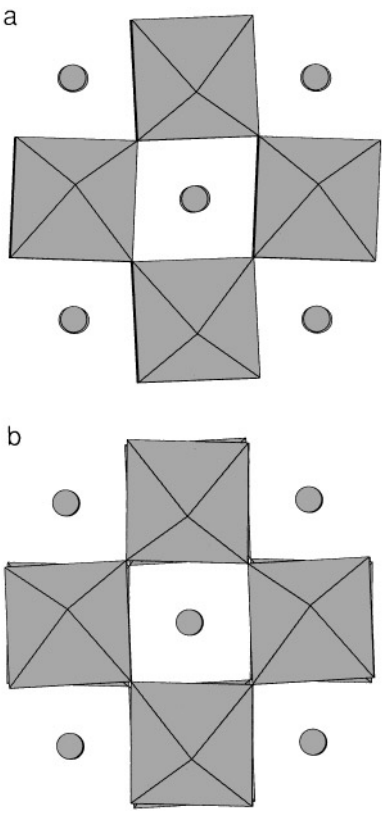

FIG. 6. Structures of (a) $LaGaO_3$ and (b) $La_{0.9}Sr_{0.1}Ga_{0.8}Mg_{0.2}O_{2.85}$ looking down the $[001]_p$ axis.

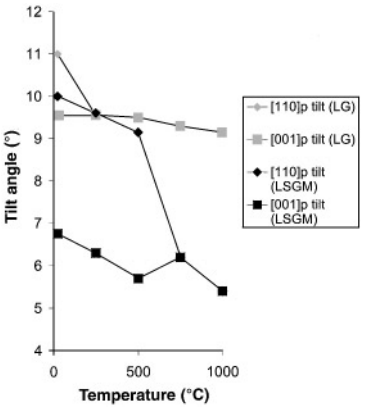

FIG. 7. Plot of GaO_6 octahedra tilt angles versus temperature for $LaGaO_3$ (LG) and $La_{0.9}Sr_{0.1}Ga_{0.8}Mg_{0.2}O_{2.85}$ (LSGM).

by 500°C, it appears as if the vacancies have become disordered over the two sites. The thermal parameters of both oxygen sites, particularly the O1 site, are higher for all temperatures than for undoped $LaGaO_3$. In addition, the thermal parameters of the cation sites are also higher for the doped system. This is expected, as a result of the disorder induced by the doping of different cations into the structure.

The fundamental differences between the GaO_6 octahedra in the two systems would be expected to have a major effect on the activation energy for the ionic conduction. In this respect it is interesting to note the observed change in activation energy for conduction for $La_{0.9}Sr_{0.1}Ga_{0.8}Mg_{0.2}O_{2.85}$ in the region 600–700°C (Fig. 9). In this study we have shown the existence of a second phase transition in this system from monoclinic (pseudo-rhombohedral) to rhombohedral, which occurs somewhere in the region 500–750°C, i.e., at a similar temperature to the change in activation energy. We can therefore propose that the change in activation energy may be related to the phase change. If we consider the structural changes that are occurring at the phase transition, we can see that the major change is equalization of the tilt angles (Fig. 7). This results in a large drop in the $[110]_p$ tilt, with a small increase in the $[001]_p$ tilt. In Fig. 10 we show a space-filling model for an ideal undistorted perovskite, ABO_3, with one of the oxygen atoms removed. For oxygen X to move to the empty site, it must

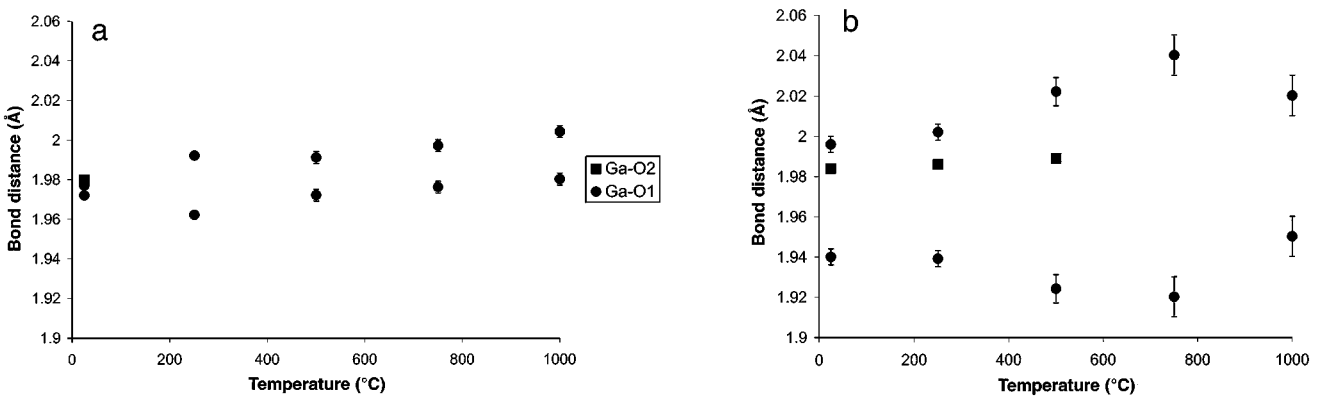

FIG. 8. Plot of Ga–O bond distance versus temperature for (a) $LaGaO_3$ and (b) $La_{0.9}Sr_{0.1}Ga_{0.8}Mg_{0.2}O_{2.85}$.

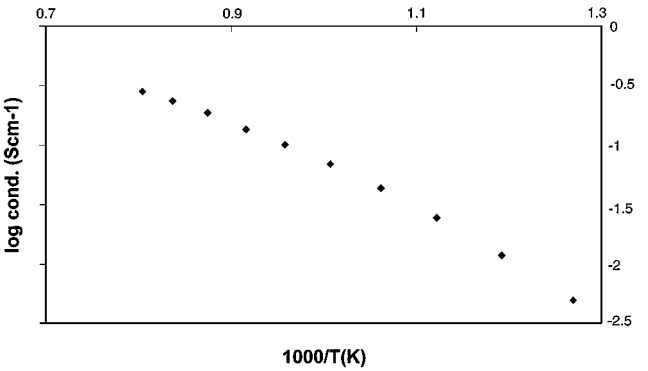

FIG. 9. Plot of log(conductivity) versus $1/T$ for $La_{0.9}Sr_{0.1}Ga_{0.8}Mg_{0.2}O_{2.85}$.

pass through the bottleneck defined by two A atoms and one B atom (the triangle shown in Fig. 10). If the system is undistorted, the bottleneck is most open, with the oxygen passing through normal to the triangle of atoms. As soon as the octahedra are tilted, the direction of passage is displaced from the normal, causing the bottleneck to be more restricted. We would therefore expect that the easiest migration of the oxygen ions and therefore lowest activation energy would be observed for the smallest tilt angle. The large reduction in the $[110]_p$ tilt angle at the monoclinic (pseudo-rhombohedral) $\rightarrow$ rhombohedral phase transition may therefore explain the observed drop in activation energy. This explanation is also supported by the observation that doping $La_{0.9}Sr_{0.1}Ga_{0.8}Mg_{0.2}O_{2.85}$ with smaller rare earths such as Nd reduces the oxide ion conduction. The smaller size of Nd would be expected to increase the tilting of the GaO_6 octahedra and so might be expected to raise the activation energy. The increase in the tilt angles as the rare earth size is reduced is supported by a study of $NdGaO_3$, $PrGaO_3$, and $LaGaO_3$ by Marti *et al.* (7), and a higher activation energy has been observed for doped $NdGaO_3$ compared to $LaGaO_3$ ($Nd_{0.9}Ca_{0.1}Ga_{0.95}Mg_{0.05}O_{3-x}$, 0.88 eV; $La_{0.9}Sr_{0.1}Ga_{0.8}Mg_{0.2}O_{3-x}$, 0.79 eV).

Further structural studies of samples with different compositions are planned to enhance our understanding of this interesting system.

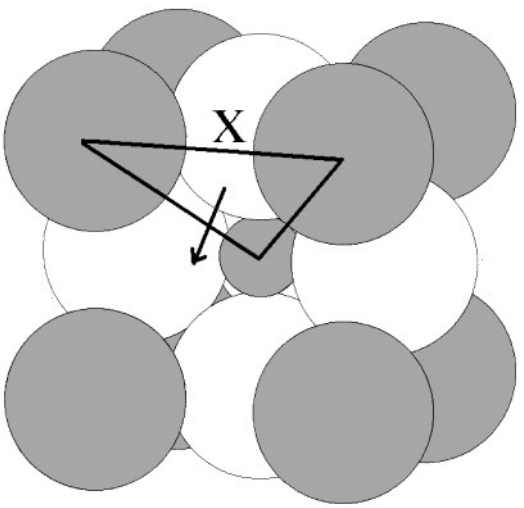

FIG. 10. Space-filling model for an undistorted perovskite ABO_3 (A, large dark spheres; O, large light spheres; B, small dark spheres), with one of the oxygen atoms moved. The oxygen atom marked X must move through the bottleneck defined by the triangle ($2A + 1B$) to reach the vacant site.

CONCLUSIONS

This powder neutron diffraction study has shown significant differences between the structures of undoped $LaGaO_3$ and $La_{0.9}Sr_{0.1}Ga_{0.8}Mg_{0.2}O_{2.85}$, which exhibits high oxide ion conductivity at elevated temperatures. In agreement with previous studies, $LaGaO_3$ is orthorhombic at room temperature and transforms to rhombohedral symmetry between 25 and 250°C. In contrast, the room temperature structure of $La_{0.9}Sr_{0.1}Ga_{0.8}Mg_{0.2}O_{2.85}$ is monoclinic, and this material exhibits two phase transitions between 25 and 1000°C, rather than one as observed for $LaGaO_3$. A possible explanation for the change in activation energy for conduction in the region 650–700°C has been presented in terms of a reduction in the GaO_6 tilting at the phase transition from monoclinic (pseudo-rhombohedral) to rhombohedral. In conclusion, these studies have shown that $La_{0.9}Sr_{0.1}Ga_{0.8}Mg_{0.2}O_{2.85}$ is a much more complex system than initially thought, showing a wealth of structural chemistry, which is important to digest to help in our understanding of the oxide ion conduction in this material as well as perovskites in general.

ACKNOWLEDGMENTS

We thank EPSRC, the MOD, and the Nuffield Foundation for financial support. We also thank K. S. Knight (Rutherford Appleton Laboratory) for help with the collection of the powder neutron diffraction data on the HRPD station at ISIS.

REFERENCES

1. T. Ishihara, H. Matsuda, and Y. Takita, *J. Am. Chem. Soc.* **116,** 3801 (1994).
2. T. Ishihara, H. Matsuda, and Y. Takita, *Solid State Ionics* **79,** 147 (1995).
3. M. Feng, J. B. Goodenough, K. Huang, and C. Milliken, *J. Power Sources* **63,** 47 (1996).
4. T. Ishihara, H. Minami, H. Matsuda, H. Nishiguchi, and Y. Takita, *Chem. Commun.* 929 (1996).
5. T. Moeller and G. L. King, *J. Am. Chem. Soc.* **75,** 6060 (1953).

6. M. Sundberg, P.-E. Werner, M. Westdahl, and K. Mazur, *Mater. Sci. Forum.* **166,** 795 (1994).
7. W. Marti, P. Fischer, F. Altorfer, H. J. Scheel, and M. Tadin, *J. Phys. Condens. Matter* **6,** 127 (1994).
8. J. Drennan, V. Zelizko, D. Hay, F. T. Ciacchi, S. Rajendran, and S. P. S. Badwal, *J. Mater. Chem.* **7,** 79 (1997).
9. J. C. Matthewman, P. Thompson, and P. J. Brown, *J. Appl. Crystallogr.* **15,** 167 (1982).
10. P. J. Brown and J. C. Matthewman, Rutherford Appleton Laboratory Report RAL-87-010, 1987.
11. C. Ritter, P. G. Radaelli, M. R. Lees, J. Barratt, G. Balakrsihnan, and D. McK. Paul, *J. Solid State Chem.* **127,** 276 (1996).
12. J. Kobayashi, Y. Tazoh, M. Sasaura, and S. Miyazawa, *J. Mater. Res.* **6,** 97 (1991).
13. R. D. Shannon, *Acta Crystallogr. Sect. A* **32,** 751 (1976).
14. A. M. Glazer, *Acta Crystallogr. Sect. A* **31,** 756 (1975).